Continuum Multi-Dielectric Treatment of Membrane Fluctuations with Embedded Charges

Michael B. Partenskii,[1] Gennady V. Miloshevsky,[1,2] Ahmed Hassanein[2] and Peter C. Jordan[1]

[1]Department of Chemistry, Brandeis University, Waltham, MA, USA

[2]School of Nuclear Engineering, Purdue University, West Lafayette, IN, USA

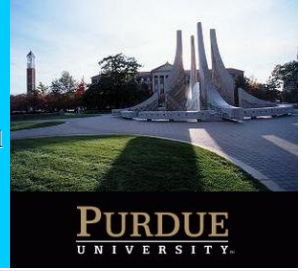

Abstract

Stabilization of protein charges due to their interaction with membrane fluctuations is a subject of growing interest, especially due to possible implications for voltage gating. Two complementary mechanisms governing charge-fluctuation interactions are considered: (1) *electroelastic (EM)* [1], treating the membrane as an elastic slab (smectic bilayer model); (2) *hydrophobic* (*HM*), accounting for water penetration into the membrane's hydrophobic core with a corresponding interfacial tension contribution. In both the linear Poisson-Boltzmann equation is solved via a multi-dielectric continuum model with arbitrarily shaped membrane-water interfaces and a point charge surrounded by a "Born sphere" of low dielectric constant. The *EM* often leads to large membrane thickness perturbations, far larger than consistent with elastic model descriptions. We show that a switch from *EM* to *HM* is energetically advantageous at intermediate perturbation amplitudes. To establish the shape of the solvation cavity we apply kinetic Monte Carlo Reaction Path Following (kMCRPF) [2] with the charge's z-coordinate as the reaction coordinate. The resulting energy profile confirms that of recent MD studies [3].

Introduction

Coupling of electric fields or charges with the fluctuations of the membrane-solvent interface is important for membrane stability, electroporation, ionic transport and voltage gating [4]. We study membrane fluctuations triggered by a single charge bound within the membrane. *EM* and *HM* influences on interfacial fluctuations are considered. The energy penalties from fluctuations reflect the elastic energy of the membrane deformation (*EM*) and the "interfacial tension" contribution (*HM*). Stabilization arises from water shielding of the charges' electric field, generating the ponderomotive force promoting the fluctuations.

We demonstrate using kMCRPF [2] that the *EM* quite typically predicts an instability leading to the charge-solvated state and the deformations far beyond the elastic limit. This indicates that at some point *EM* fluctuations must switch to *HM* ones. Fluctuations in the *HM* model are investigated using an extended family of parameterized shapes that sample a wide range of solvated states. Preliminary results indicate that fluctuations typically arise due to electroelastic interaction (*EM*), which then trigger the massive water penetration governed by the *HM*.

Computational Model

Source-free Poisson-Boltzmann equation, $\phi_\delta = \phi - \phi_c$

$\nabla \cdot \varepsilon \nabla \phi_\delta = -\nabla \cdot (\varepsilon - \varepsilon_p) \nabla \phi_c$ where $\phi_\delta = \phi - \phi_c$, ε_p - dielectric constant near the charge, ϕ_c - the coulombic potential calculated analytically from $\varepsilon_p \nabla^2 \phi_c = -4\pi q$ [5].

Inside the charge sphere $\varepsilon = \varepsilon_p = 1$, and the Poisson-Boltzmann equation is $\varepsilon_p \nabla^2 \phi_\delta = 0$

Outside the charge sphere ϕ_c is well defined; thus

- singularities due to point charges are eliminated
- reaction field potentials are computed directly

Computational Domain

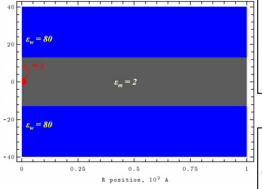

Cylindrical geometry: r = 0 ÷ 100 Å; z = -40 ÷ 40 Å; mesh step: 0.2 Å; 501 × 401 grid points

Boundary Conditions

$\phi_\delta = \phi - \phi_c = 0 - \dfrac{q}{\varepsilon_p \rho(r_b, z_b)}$, where

$\rho(r_b, z_b) = \sqrt{(r_b - r_0)^2 + (z_b - z_0)^2}$

(r_0, z_0) - the r and z coordinates of the point charge

(r_b, z_b) - the r and z coordinates of the boundary points in the computational domain

Electrostatic Energy

$E_{elect} = \dfrac{1}{2} q \phi_\delta(r_0, z_0)$, with

$\phi_\delta(r_0, z_0)$ - the reaction field potential at location of the point charge

Elastic Energy

$E_{elast} = 2\pi \int_0^R w(r) r dr$, where $w(r) = a(z_1(r) + z_2(r))^2 + b\left(LU_1(r)^2 + LU_2(r)^2\right)$

with $a = E_s / (2h^2)$ and $b = K_c / 4$.

For DOPC: $E_s = 0.45\ kT/Å^2$, $K_c = 4.83\ kT$ and $h = 26\ Å$

For DMPC: $E_s = 0.35\ kT/Å^2$, $K_c = 13.5 \div 26.6\ kT$ and $h = 25.2\ Å$ (both for 300 K)

Gaussian Shape	Hertzian Shape
$z_i(r) = u_i \exp(-r^2/\lambda_i^2)$	$z_i(r) = u_i Kei(r/\lambda_i)/Kei(0)$
$LU_i(r) = -4u_i(\lambda_i^2 - r^2)\exp(-r^2/\lambda_i^2)/\lambda_i^4$	$LU_i(r) = u_i Ker(r/\lambda_i)/(\lambda_i^2 Kei(0))$ $\quad i = 1,2$

Hydrophobic Energy

$W_{hydro} = \gamma S$

the pore formation energy with $\gamma = 10 \div 20\ kJ/(mol \cdot nm^2)$ the interfacial tension and S the hydrophobic pore's total area.

Solution Method

- MUltifrontal Massively Parallel Solver (MUMPS) [6], an accurate direct method based on *LU* matrix factorization, is used to solve the system of linear equations, $\mathbf{Ax} = \mathbf{b}$, where $\mathbf{A}$ is an unsymmetric sparse matrix. It utilizes MPI for message passing and makes use of the BLAS, BLACS and ScaLAPACK libraries.
- Continuum Electroelastics of Membrane Electrolyte Assembly (CE-MEA) parallel code is developed in mixed Fortran 90/95 and C/C++. It is implemented by using the MPI-2 standard for parallel communications. The CE-MEA code runs on Linux or Windows Intel Clusters with 64 bit addressing.

kMC Reaction Path Following (kMCRPF)

kMCRPF [2] navigates on the energy surface, establishing minimum energy pathways and energy profiles as follows:

- Establish z_q (the charge's z-coordinate) as a reaction coordinate
- Allow only unidirectional (constrained) motion of the charge along the reaction coordinate, all other degrees of freedom are unconstrained

Degrees of Freedom

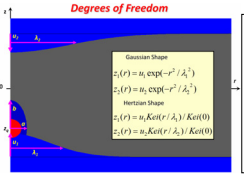

1. calculate the initial energy, E^{old}, of the system
2. perform a unidirectional move along the reaction coordinate
3. calculate the energy, E^{new}, of a new state and $\Delta E = E^{new} - E^{old}$
4. if $\Delta E \le 0$, accept a trial move; if $\Delta E > 0$, accept a trial move if $R \le \exp(-\Delta E/kT)$, where R is a random number between 0 and 1; otherwise reject it, reduce the maximum step length along the reaction coordinate and go to step 2
5. use the unconstrained Metropolis MC method to perform many MC trials relaxing the other degrees of freedom while fixing a reaction coordinate; go to step 2

u_1, u_2 and λ_1, λ_2 are the amplitudes and decay lengths of the lower and upper water plumes described either by the *EM* or the *HM*; *a* and *b* are the axis lengths of the elliptic water plume described by the *HM*; for the case of the ellipse with cones the upper and lower cone's base lengths are degrees of freedom; z_q is the charge's z-coordinate

Parameterized Shapes of Water Pores

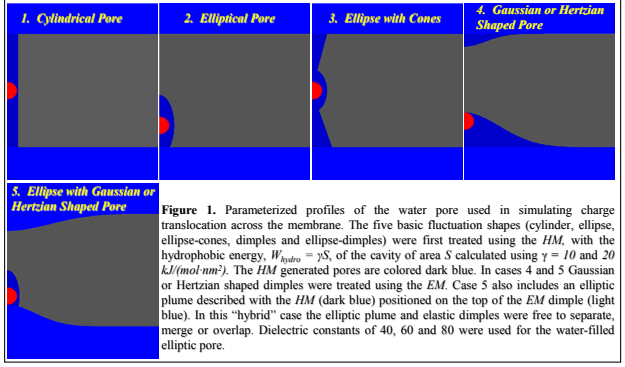

Figure 1. Parameterized profiles of the water pore used in simulating charge translocation across the membrane. The five basic fluctuation shapes (cylinder, ellipse, ellipse-cones, dimples and ellipse-dimples) were first treated using the *HM*, with the hydrophobic energy, $W_{hydro} = \gamma S$, of the cavity of area *S* calculated using $\gamma = 10$ and $20\ kJ/(mol \cdot nm^2)$. The *HM* generated pores are colored dark blue. In cases 4 and 5 Gaussian or Hertzian shaped dimples were treated using the *EM*. Case 5 also includes an elliptic plume described with the *HM* (dark blue) positioned on the top of the *EM* dimple (light blue). In this "hybrid" case the elliptic plume and elastic dimples were free to separate, merge or overlap. Dielectric constants of 40, 60 and 80 were used for the water-filled elliptic pore.

kMC Reaction Path Following of the Charge across the Membrane

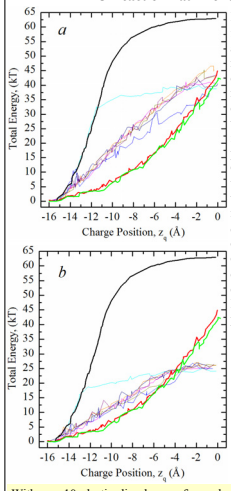

Figure 2. Total energy profiles as a function of charge position for DOPC. The charge was limited to unidirectional moves across the membrane via kMCRPF; the axial position, z_q, is the reaction coordinate. After each accepted move the other degrees of freedom were relaxed using 200 MC trials. All energies are relative to the energy of the unperturbed membrane with the charge immobilized in bulk water (z_q = -16 Å). The charge was tracked to mid-membrane (z_q = 0 Å). The thick black curve illustrates the energy for a flat membrane (no water dimples or plumes). Thick red and green curves are energies for elastic Gaussian and Hertzian shaped dimples, respectively, calculated using the *EM* model. The thin curves are energy profiles for the water plume shapes shown in Fig. 1 and described by the *HM* model with $\gamma = 20$ (***a***) and $\gamma = 10$ (***b***). The cyan and blue curves correspond to cylindrical and joined ellipse-cone shapes. At a γ-dependent z_q, charge entry into the membrane creates a cylindrical pore of fluctuating radius (case 1), which remains open as the charge moves toward mid-membrane. The other five closely spaced curves are elliptical (case 2), and Gaussian or Hertzian shaped dimples without (case 4) and with the elliptical plume (case 5). $\varepsilon \equiv 80$ for these water-filled pores.

Main observations:

- The elastic (water dimples) fluctuations significantly reduce the energy barrier (by ~20 kT) and qualitatively changes the energy profile from a "wide-bell" (black curve) to "triangular" shape (red and green curves).
- With $\gamma = 20$ no energetic advantage accrues to variably shaped water plumes (*HM*) as compared with elastic water dimples described by the *EM* (Fig. 2a). For larger γ an increase in the energy barrier is expected.

With $\gamma = 10$ elastic dimples are favored near the membrane surface and plumes become favored as the charge penetrates the membrane (the barrier drops ~18 kT) showing that the *HM* contributes significantly for $z_q > -5$ Å (Fig. 2b). For smaller γ this switch could occur even closer to the membrane-water interface.

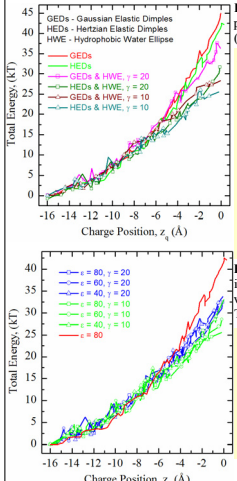

Figure 3. Total energy profiles as functions of charge's z_q position in a DOPC membrane for the "hybrid" fluctuations (Fig. 1, case 5).

Main observations:

- Translocation of the charge is accompanied by both the HM (elliptic water plume) and EM (elastic dimples) fluctuations along the whole pathway. Close to mid-membrane the charge is mainly solvated by the water plume.
- For $z_q > -6$ Å HM fluctuation reduces the total energy relative to the case of a purely elastic component; Hertzian-shaped dimples are favored relative to Gaussian-shaped dimples.
- The energy barrier drops with deceasing the elliptic water plume's tension constant.
- Elastic fluctuations promote water penetration; thus both mechanisms typically participate in solvating the ion.

Figure 4. Total energy profiles as functions of charge position in a DOPC membrane for "hybrid" fluctuations. The effects of varying water plume ε and interfacial tension are illustrated. The red curve is the water plume-free case.

Main observations:

- For $-16 < z_q < -6$ Å, the energy profiles in Figs. 3 and 4 closely mimic those of Fig. 2 (red and green curves, elastic dimples); for $z_q > -6$ Å, the Figs. 3 and 4 energy barriers are considerably reduced due to water plume influences.
- The energy barrier is higher for a water plume with smaller ε and larger γ; the barrier lies in an ~10 kT range, depending on the parameters.

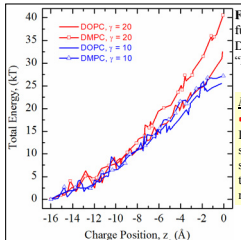

Figure 5. Total energy profiles as functions of charge position in DOPC and DMPC membranes for "hybrid" fluctuations. Pore ε is 80.

Main observation:

- The energy barrier is lower for DOPC (presumably) due to the smaller elastic bending modulus; smaller tension constant reduces the energy barrier in both membranes.

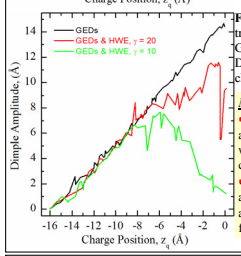

Figure 6. Averaged (over 200 MC trials for each z_q) amplitudes of Gaussian-shaped elastic dimples in DOPC membranes as functions of charge position.

Main observations:

- For $z_q > -6$ Å dimple amplitudes are greatly reduced due to the water plume's influence on charge solvation.
- The tension constant crucially affects system behavior: for low γ an elliptic water-filled pore forms for a charge near mid-membrane.

Conclusions

- The transmembrane transition energy barrier is strongly affected by fluctuations and differs significantly from the classical picture, a planar (unperturbed) membrane. The optimized barrier shape alters from a "wide-bell" to a "triangular" shape (Fig. 2). Similar behavior was observed in atomistic MD simulations of a charged arginine side chain translated across a lipid bilayer [3].
- For $-16 < z_q < -6$ Å the charge is mainly solvated by the elastic dimple (*EM*) with a small elliptic water plume attached to the dimple's head. For $z_q > -6$ Å its solvation heavily involves the water plume (*HM*), whose formation is promoted by the elastic fluctuations The translocation process is strongly affected by the interplay between the elastic and hydrophobic fluctuations.
- *HM* fluctuations can be strongly promoted by elastic influences, especially as the charge approaches mid-membrane. Fluctuations can reduce the barrier to ~25-30 kT (Figs. 3-5), while the corresponding barrier for a planar membrane is ~63 kT (Fig. 2). The energy barrier from MD simulations [3] was ~28.5 kT.
- The choice of parameters describing the water plume (dielectric and tension constants) strongly affects system behavior. The transition energy barrier drops with decreasing "interfacial tension." Estimates of γ vary widely, depending on interaction between hydrophobic bilayer organizational forces and curvature energy due to lipid headgroup tilt, attenuating hydrophobic influences [7].

References

1. M. B. Partenskii et al., *Israel J. Chem.* **47**, 385 (2007).
2. G. V. Miloshevsky & P. C. Jordan, *J. Chem. Phys.* **122**, 214901 (2005).
3. S. Dorairaj & T. W. Allen, *PNAS* **104**, 4943 (2007).
4. Long et. al., *Science*, 309, 897 (2005); *Nature*, **450,** 376 (2007).
5. Z. Zhou et al., *J. Comp. Chem.* **11,** 1344 (1996).
6. P. R. Amestoy et al., *Parallel Computing* **32**, 136 (2006).
7. P. A. Bachier et al., *Biophys. J.* **92**, 4344 (2007).

Acknowledgement

Work supported by the NIH under grant GM-28643.
Computational resources provided by the NCSA under grant MCB080096N.